

Introduction of Three-Dimensional Extrinsic Defects into Colloidal Photonic Crystals

Qingfeng Yan, Zuocheng Zhou, and X. S. Zhao*

Department of Chemical and Biomolecular Engineering,
National University of Singapore, 10 Kent Ridge Crescent,
Singapore 119260

Received February 19, 2005

Revised Manuscript Received May 5, 2005

Photonic crystals (PCs) or photonic band gap (PBG) materials have attracted rapidly growing interest because of their potential applications in photonics.^{1,2} Self-assembly of colloidal microspheres offers a simple and inexpensive route to three-dimensional (3D) PCs.³ Over the past decade, various methods have been demonstrated to fabricate colloidal PCs.^{4–7} Particular efforts have been made at minimization of the presence of intrinsic defects such as dislocations and cracks to achieve perfect and large-scale colloidal crystals.^{8–10} However, the incorporation of different kinds of extrinsic defects such as planar, line, and point defects into the colloidal PCs is also of paramount importance. Device applications of PCs, such as low-loss waveguides, optical cavities, zero-threshold microlasers, light-emitting diodes, optical switches, all-optical transistors, and tunable filters all require an exact placement of well-defined defects in the interior of the PCs.¹¹ Defect engineering for self-assembled PCs has thus been of great research interest.^{12–18} In addition, photonic crystal heterostructures with multiple photonic band gaps provide the potential of controlling and modulating the flow of light more elaborately.¹⁹

Template-directed self-assembly of colloidal spheres has been widely used to produce size-controlled colloidal

clusters,^{20–22} oriented colloidal crystals,^{23,24} and photonic crystal heterostructures.²⁵ Most of these template patterns are defined on a flat solid substrate using lithography techniques.^{23,25–31} Here, we show that various patterns can be constructed on the surface of a colloidal crystal film (host opal). By directed self-assembly of another kind of colloidal crystal (guest opal) within these patterns, followed by sequential growth of the host opal, one can embed 3D extrinsic defects with desired shapes in the interior of a self-assembled colloidal PC.

The fabrication procedure is schematically illustrated in Figure 1. Monodisperse silica colloidal microspheres with a diameter of 0.39 μm , which were synthesized using the Stöber-Fink-Bohn method,³² were assembled on a silicon substrate with a vertical deposition method⁷ to form a colloidal crystal film. The thickness of the film can be precisely controlled with manipulating the concentration of the silica colloidal suspension. The silica opal film was slightly annealed at 450 °C for 3 h to enhance the mechanical integrity. Because of the low annealing temperature employed, the colloidal crystal film retained its original crystal-line structure and no cracks were formed upon the annealing process. After spin-coating of a photoresist layer (either AZ P4620 or AZ 5214, Clariant Pte Ltd), conventional photolithography technique was used to construct a variety of linear channels on the surface of the silica opal film (see Supporting Information for the details of the photolithography process). Then, vertical deposition or spin-coating was employed to grow polystyrene (PS) colloidal crystal (guest opal) within the channels. The PS spheres were synthesized using an emulsifier-free emulsion polymerization technique.³³ The detailed experimental description of the fabrication of the PS guest opal can be found in the Supporting Information. After drying at room temperature followed by heat treatment at 100 °C for 10 min to slightly anneal the PS guest opal, the photoresist was removed with ethanol. Subsequently, vertical deposition was carried out again to re-grow the host silica colloidal crystal, resulting in a 3D PS guest opal strip embedded in the interior of the silica host opal. Images were

* To whom correspondence should be addressed. Fax: 65-67791936. E-mail: chezxs@nus.edu.sg.

- (1) Yablonovitch, E. *Phys. Rev. Lett.* **1987**, *58*, 2059.
- (2) John, S. *Phys. Rev. Lett.* **1987**, *58*, 2486.
- (3) Xia, Y. N. *Adv. Mater.* **2001**, *13*, 369.
- (4) Yan, Q.; Zhou, Z.; Zhao, X. S. *Langmuir* **2005**, *21*, 3158.
- (5) Park, S. H.; Xia, Y. *Langmuir* **1999**, *15*, 266.
- (6) Zhou, Z.; Zhao, X. S. *Langmuir* **2004**, *20*, 1524.
- (7) Jiang, P.; Bertone, J. F.; Hwang, K. S.; Colvin, V. L. *Chem. Mater.* **1999**, *11*, 2132.
- (8) Wong, S.; Kitaev, V.; Ozin, G. A. *J. Am. Chem. Soc.* **2003**, *125*, 15589.
- (9) Jiang, P.; McFarland, M. J. *J. Am. Chem. Soc.* **2004**, *126*, 13778.
- (10) Chabanov, A. A.; Jun, Y.; Norris, D. J. *Appl. Phys. Lett.* **2004**, *84*, 3573.
- (11) Joannopoulos, J. D.; Meade, R. D.; Winn, J. N. *Photonic Crystals: Molding the Flow of Light*, 1st ed.; Princeton University Press: Princeton, NJ, 1995.
- (12) Wostyn, K.; Zhao Y.; Schaetzen G.; Hellenmans L.; Matsuda N.; Clays K.; Persoons A. *Langmuir* **2003**, *19*, 4465.
- (13) Palacios-Lidón, E.; Galisteo-López J. F.; Juárez B. H.; López C. *Adv. Mater.* **2004**, *16*, 341.
- (14) Tétreault, N.; Mihi, A.; Míguez, H.; Rodríguez, I.; Ozin, G. A. *Adv. Mater.* **2004**, *16*, 346.
- (15) Pradhan, R. D.; Tarhan, I. I.; Watson, G. H. *Phys. Rev. B* **1996**, *54*, 13721.
- (16) Lee, W.; Pruzinsky, A.; Braun, P. V. *Adv. Mater.* **2002**, *14*, 271.
- (17) Yan, Q.; Zhou, Z.; Zhao, X. S.; Chua, S. J. *Adv. Mater.* **2005**, in press.
- (18) Ferrand, P.; Egen, M.; Zentel, R.; Seekamp, J.; Romanov, S. G.; Torres, C. M. S. *Appl. Phys. Lett.* **2003**, *83*, 5289.
- (19) Romanov, S. G.; Yates, H. M.; Pemble, M. E.; De La Rue, R. M. J. *Phys.: Condens. Matter* **2000**, *12*, 8221.

- (20) Yin, Y.; Lu, Y.; Gates, B.; Xia, Y. *J. Am. Chem. Soc.* **2001**, *123*, 8718.
- (21) Xia, Y.; Yin, Y.; Lu, Y.; McLellan, J. *Adv. Funct. Mater.* **2003**, *13*, 907.
- (22) Schaak, R. E.; Cable, R. E.; Leonard, B. M.; Norris, B. C. *Langmuir* **2004**, *20*, 7293.
- (23) Zhang, J.; Alsayed, A.; Lin, K. H.; Sanyal, S.; Zhang, F.; Pao, W.-J.; Balagurusamy, V. S. K.; Heiney, P. A.; Yodh, A. G. *Appl. Phys. Lett.* **2002**, *81*, 3176.
- (24) Yin, Y.; Li, Z.-Y.; Xia, Y. *Langmuir* **2003**, *19*, 622.
- (25) Yang, S. M.; Míguez, H.; Ozin, G. A. *Adv. Funct. Mater.* **2002**, *12*, 425.
- (26) Yin, Y.; Xia, Y. *Adv. Mater.* **2001**, *13*, 267.
- (27) van Blaaderen, A.; Ruel, R.; Wiltzius, P. *Science* **1997**, *385*, 321.
- (28) Yang, S. M.; Ozin, G. A. *Chem. Commun.* **2000**, 2507.
- (29) Xia, D.; Biswas, A.; Li, D.; Brueck, S. R. J. *Adv. Mater.* **2004**, *16*, 1427.
- (30) Xia, D.; Brueck, S. R. J. *Nano Lett.* **2004**, *4*, 1295.
- (31) Ye, Y.-H.; Badilescu, S.; Truong, V.-V. *Appl. Phys. Lett.* **2001**, *79*, 872.
- (32) Stöber, W.; Fink, A.; Bohn, E. *J. Colloid Interface Sci.* **1968**, *26*, 62.
- (33) Shim, S. E.; Cha, Y. J.; Byun, J. M.; Choe, S. J. *Appl. Polym. Sci.* **1999**, *71*, 2259.

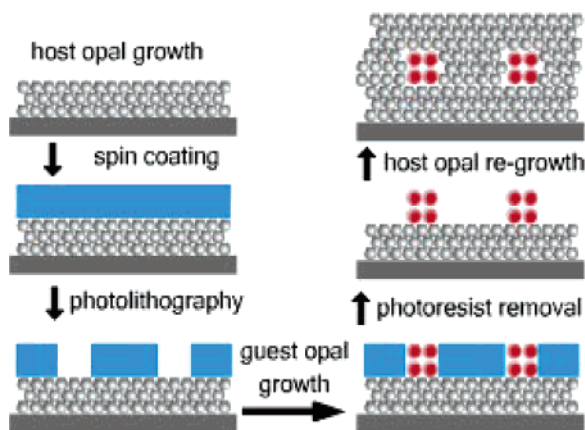


Figure 1. Schematic illustration of introducing three-dimensional (3D) extrinsic defects into self-assembled colloidal PCs.

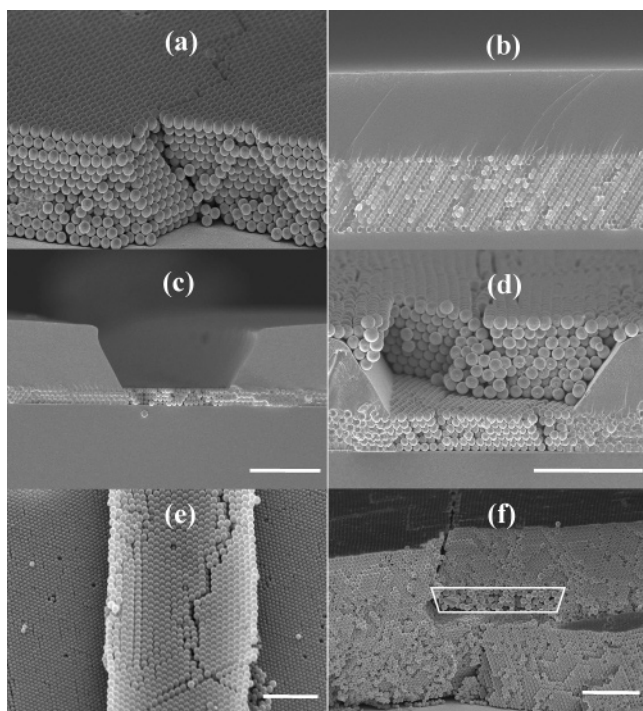


Figure 2. Scanning electron microscopy (SEM) images of (a) a silica colloidal crystal film ($0.39 \mu\text{m}$ in diameter), (b) after spin-coating of a layer of photoresist, (c) a photoresist linear channel patterned on the surface of the silica colloidal crystal film, (d) PS guest opal ($0.56 \mu\text{m}$ in diameter) strip in the channel, (e) after removal of photoresist, and (f) a PS guest opal strip embedded in the interior of the silica colloidal photonic crystal (host opal). The white rectangle highlights the embedded guest opal. All scale bars are $5 \mu\text{m}$.

acquired using a field emission scanning electron microscopy (FESEM, JEOL JSM-6700F) and a scanning electron microscopy (SEM, JEOL JSM-5600LV).

The SEM images shown in Figure 2 demonstrate the opal structures obtained in each step. Figure 2a shows a silica opal film produced using the vertical deposition method. It is seen that the film possesses a face-centered cubic (fcc) close-packed structure with the (111) plane parallel to the substrate surface. Figure 2b shows a side view of the silica opal film after spin-coating of a $5\text{-}\mu\text{m}$ layer of photoresist AZ P4620. The thickness of the photoresist layer can be controlled by the spinning speed and time. It is also dependent upon the photoresist properties. (For example, with photoresist AZ 5214, which has a lower viscosity, a

photoresist layer of less than $1 \mu\text{m}$ was obtained using a spinning speed of 5000 rpm for 0.5 min, while when photoresist AZ P4620 was used, a spinning speed of 5000 rpm for 0.5 min resulted in a photoresist layer of about $7 \mu\text{m}$ in thickness. When a multiple-coating process was used, photoresist layers thicker than $10 \mu\text{m}$ were also obtained). During the spin-coating process, the photoresist penetrated the voids between the silica colloidal spheres as revealed by the SEM image shown in Figure 2b. After photolithography and development, micrometer-scale ($9 \times 5 \mu\text{m}$) channels were constructed on the top of the silica opal film as demonstrated by the SEM image of Figure 2c. The guest PS opal was fabricated with the same vertical deposition method. The silica film with patterned channels was dipped in a PS colloidal aqueous suspension in a way that the linear channels were oriented perpendicular to the liquid surface of the suspension. A proper PS colloidal suspension concentration must be used to ensure PS colloids to crystallize only in the channels. As can be seen from Figure 2d, both the PS colloidal crystal ($0.56 \mu\text{m}$) within the $9\text{-}\mu\text{m}$ -wide channel and the underneath silica colloidal crystal ($0.39 \mu\text{m}$) are well-structured. Figure 2e shows the PS colloidal crystal strip loaded on the top of the silica colloidal crystal film after the photoresist was removed. Dipping in ethanol ensured the complete removal of the photoresist on the top of the silica colloidal crystal film, as well as those penetrating the underneath silica colloidal crystals. The well-defined architecture of the PS colloidal crystal strip and the close-packed hexagonal surface plane of the silica opal underneath the PS opal strip are clearly seen. It can also be observed that the PS guest opal strip contains some cracks, which are likely due to the shrinkage of the self-assembled PS spheres during the drying process. After re-growth of another layer of silica colloidal crystal, a 3D PS colloidal crystal strip fully embedded in the interior of the silica colloidal crystal was obtained, which can be seen from Figure 2f. Figure S1 in the Supporting Information shows the enlarged section of the PS guest opal strip surrounded by the silica host opal. It is hard to distinguish the interface between the original silica opal and the re-grown one, indicating a perfect periodicity of the 3D ordered structure inherited when the top layer silica colloidal crystal was grown on the surface of the original silica opal film.

In addition to the vertical deposition method, the spin-coating method^{29,30,34} was also utilized to fabricate guest PS opals. The spin-coating technique is especially useful for fabrication of guest colloidal crystal from spheres with a larger diameter or having a higher density (i.e., silica), for which the conventional vertical deposition method is not effective because of particle sedimentation. The concentration of the PS colloidal suspension and the spin speed were optimized to ensure the crystallization of the PS colloids to take place only within the channels. As an example, Figure 3 shows a 3D PS colloidal crystal (the diameter of the PS spheres was $1.1 \mu\text{m}$) strip embedded in a silica colloidal crystal (the diameter of the silica spheres was $0.39 \mu\text{m}$). The structural order of the PS guest opal fabricated using the spin-coating method can be clearly seen.

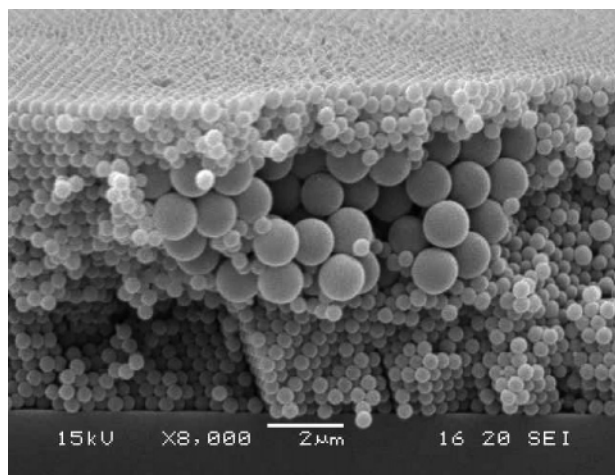


Figure 3. A three-dimensional PS colloidal crystal ($1.1 \mu\text{m}$ in diameter) strip embedded in a silica colloidal crystal ($0.39 \mu\text{m}$ in diameter). The PS guest opal was fabricated by means of the spin-coating technique.

Besides straight linear channels, other complex channels such as S-bend, Y-branch, X-cross, and ring-like channels have also been patterned on the surface of silica colloidal crystal films following the route described in this work. Thus, guest opal with a desired shape can be introduced into 3D self-assembled systems with the same method. As an example, Figure 4a shows the SEM image of a Y-branch channel patterned on the surface of a silica opal film. The high-resolution SEM image of the branch section (Figure 4b) and the cross-sectional view (Figure 4c) clearly illustrate the well-defined channels and the hexagonal-packed surface plane of the silica opal underneath the channels. A Y-shape PS guest opal strip loaded on the silica colloidal crystal film, which was directly grown within the Y-branch channel, can be seen from Figure 4d. The insets in Figure 4d show the top view of the PS guest opal (top) and the silica host opal (bottom). The PS guest opal strip was prepared using the spin-coating method. The poor ordering of the PS colloidal spheres (see the enlarged SEM image shown in Figure S2 in the Supporting Information) is most probably due to the incommensurability of the diameter of the PS spheres ($0.26 \mu\text{m}$) and the dimension of the channel ($4\text{-}\mu\text{m}$ wide and $2\text{-}\mu\text{m}$ height),^{31,35–37} and/or the un-optimized spin-coating parameters. An S-bend shape PS guest opal strip loaded on a silica host opal film can be seen in Figure S3 in the Supporting Information.

In summary, an effective and simple method for engineering micrometer-scale three-dimensional extrinsic defects within self-assembled colloidal photonic crystals has been demonstrated. The method combines the techniques of self-assembly of colloidal spheres, photolithography on a pre-formed colloidal crystal, template-directed colloidal crystal growth, and sequential growth of colloidal crystal. The heterostructured colloidal crystals are expected to exhibit

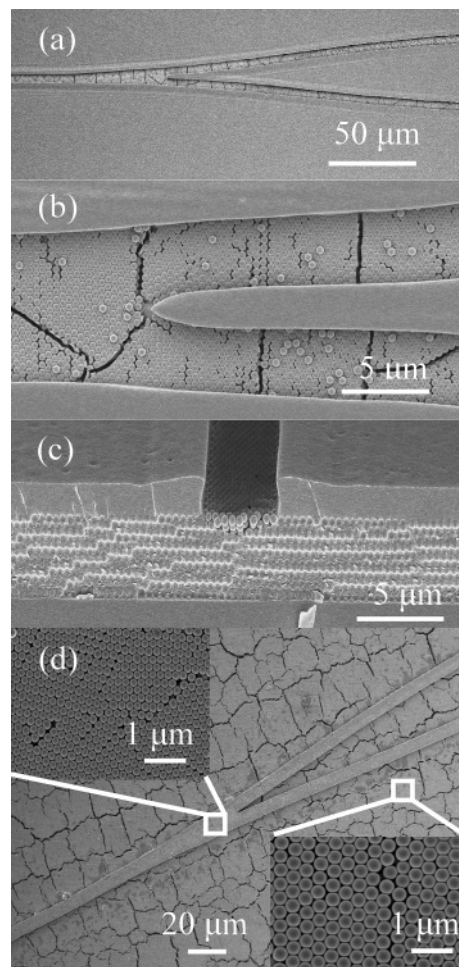


Figure 4. A Y-branch channel patterned on the surface of a silica colloidal crystal film. (a) A top view at low magnification, (b) a close view of the branch section, and (c) a cross-sectional view. (d) A Y-shape PS guest opal strip loaded on the silica host opal film. The top and bottom insets in Figure 4d illustrate the top view of the guest PS opal and the host silica opal, respectively.

elaborate optical properties because of the different PBG effects between the host and guest opal structures, offering the possibilities of controlling and modulating the flow of light. In addition, the presence of such extrinsic defects in a 3D ordered porous system may act as buried microchannels used in fluidics systems.

Acknowledgment. The authors thank the Science, Technology and Research (A*STAR) of Singapore for financial support. Dr. Teng Jinghua, Institute of Materials Research and Engineering (IMRE), Singapore, is acknowledged for his assistance with mask fabrication.

Supporting Information Available: (1) Detailed photolithography process for constructing linear channels with different height; (2) fabrication of PS guest opal within the photoresist channels; (3) an enlarged SEM image of Figure 2f; (4) an enlarged SEM image of a Y-shape PS guest opal strip loaded on a silica colloidal crystal film; (5) SEM image of an S-bend shape PS guest opal strip loaded on a silica colloidal crystal film. This material is available free of charge via the Internet at <http://pubs.acs.org>.

(35) Yin, Y.; Lu, Y.; Xia, Y. *J. Mater. Chem.* **2001**, *11*, 987.

(36) Fustin, C.-A.; Glasser, G.; Spiess, H. W.; Jonas, U. *Langmuir* **2004**, *20*, 9114.

(37) Míguez, H.; Yang, S. M.; Ozin, G. A. *Langmuir* **2003**, *19*, 3479.